Bioprocess and Biosystems Engineering (2022) 45:1799–1809
https://doi.org/10.1007/s00449-022-02786-w

RESEARCH PAPER

Facile green synthesis of Ag-doped ZnO/CaO nanocomposites with *Caccinia macranthera* seed extract and assessment of their cytotoxicity, antibacterial, and photocatalytic activity

Zahra Sabouri[1,2] · Sajjad Sabouri[3] · Samaneh Sadat Tabrizi Hafez Moghaddas[2] · Asma Mostafapour[2] · Mohammad Sadegh Amiri[4] · Majid Darroudi[1,5,6]

Received: 29 June 2022 / Accepted: 8 September 2022 / Published online: 17 September 2022

Abstract

The current paper exhibited a green method for the manufacture of Ag-doped ZnO/CaO nanocomposites (NCPs) by the usage of *Caccinia macranthera* seed extract, zinc, calcium, and silver salts solution, for the first time. The chemical structure of NCPs was studied by the FT-IR technique. The XRD pattern shows a crystallite structure with an Fm3m group space and particle size of about 23 nm. The FESEM/PSA images displayed that NCPs have uniform distribution with spherical morphology. Also, the cytotoxicity of synthesized NCPs was examined on Huh-7 cells by MTT test and the IC_{50} value was 250 ppm. Additionally, the photocatalytic activity of NCPs was investigated to the methylene blue MB dye degradation, which resulted in a removal of about 90% after 100 min. According to the results of the broth microdilution process, which was done to evaluate the antibacterial activity of NCPs towards gram-positive and gram-negative bacteria, the MIC values were in the range of 0.97–125 ppm.

Keywords Ag-doped ZnO/CaO nanocomposites · *Caccinia macranthera* seed extract · Antibacterial · Photocatalytic · Cytotoxicity

Introduction

Due to the use of various dyes (especially azo) in industries such as textiles, leather, paper, food, and cosmetics, the produced effluents by these industries are contaminated with dyes [1]. With the entry of these effluents into the environment, due to the toxic and destructive effects of dyes, the environmental conditions of surface waters, rivers, and even the soil of the region change. These changes are very dangerous for the health of humans, animals, and plants. Therefore, as much as possible, industrial effluents should be treated before entering the environment and their various pollutants should be reduced as much as possible [2, 3]. Dyes used in various industries, in addition to environmental pollution (water and soil), become very dangerous, carcinogenic, and toxic compounds over time and through various chemical processes [4, 5]. Most dyes are resistant to heat, light, as well as biodegradation and are not easily removed. Therefore, they can stay in the environment for a long time. Methylene blue (MB) is an important aromatic chemical cation dye in the textile industry and is soluble in water [6]. Effluents containing dyes such as MB are hazardous to ecosystems and public health; these substances may affect the light activity of aquatic plants, and increase suspended solids, and water turbidity by reducing light penetration [7]. With the help of conventional purification methods, these compounds cannot be separated from the medium. Various methods such

✉ Majid Darroudi
darroudim@mums.ac.ir; majiddarroudi@gmail.com

1 Department of Medical Biotechnology and Nanotechnology, Faculty of Medicine, Mashhad University of Medical Sciences, Mashhad, Iran

2 Medical Toxicology Research Center, Faculty of Medicine, Mashhad University of Medical Sciences, Mashhad, Iran

3 Civil Engineering Department, Faculty of Engineering, Yazd University, Yard, Iran

4 Department of Biology, Payame Noor University, Tehran, Iran

5 Nuclear Medicine Research Center, Mashhad University of Medical Sciences, Mashhad, Iran

6 Department of Basic Medical Sciences, Neyshabur University of Medical Sciences, Neyshabur, Iran

as the use of coagulants, oxidizing agents, optical catalytic processes, and the use of various filters and membranes for the separation of dyes have been used, which have disadvantages such as high cost and continuous need for oxidizing and coagulating agents [8]. In addition, the lack of removal of high-yield dyes is one of their disadvantages. The most efficient and best way to remove the dye is to use different adsorbents that through the adsorption process cause the dye to be transferred to the stationary phase (adsorbent). Features of this method include recycling the adsorbent and reusing it, low cost, simplicity of the method, and its design [9]. So far, many nanomaterials have been used to remove dyes from aquatic environments, including TiO_2, ZnO, MgO, and NiO, which have advantages such as a simple preparation method, relatively low cost, separation of the adsorbent from the aqueous medium, and at the same time have a high absorption capacity [3, 10, 11]. On the other hand, surface modification of nanomaterial was given a lot of focus to create biocompatible substances for wastewater treatment, pollutant removal, targeted distribution, antibacterial, and anticancer application [12–15]. Thus, various researches were informed on the employment of nanomaterials for the treatment of polluted water [16, 17]. Because of their high surface area, nanomaterials can have various applications such as sensors [18], wastewater treatment, antibacterial, and drug carriers [19–22]. Recently, nanocomposites were identified as one of the most notable materials in biological applications due to their high biocompatibility, economic benefits, and low toxicity, as well as their antibacterial and anticancer attributes [23–26]. In recent decades, not only the selection of materials that are non-toxic and low cost should be considered, rather the synthesis method plays an essential role in the development of newer materials suitable for health care technology. According to the reports, various research communities have synthesized nanocomposites using the green method and investigated their antimicrobial activity and cytotoxicity. In 2022, Sabouri et al. reported Ag-doped ZnO/MgO NCPs synthesis using green chemistry and also investigated their cytotoxicity effects on Huh-7 cell lines [25]. In 2018, Revathi et al. reported CdO–ZnO–MgO nanocomposites synthesis and studied its antibacterial activity [27]. In 2022, Hosny et al. reported Ag/ZnO@Biohar nanocomposite synthesis and also examined their antibacterial and antioxidant activities [28]. In 2019, Panchal et al. reported ZnO/MgO Nanocomposites synthesis and also examined their photocatalytic and antibacterial activities [20].

However, nanocomposite combinations engrossed the focus of many because of their unique attributes containing low toxicity and high stability. Different procedures were applied for the synthesis of these nanomaterials, such as sol–gel [29], microwave [30], hydrothermal [31], and co-precipitation [32] which contain chemical solvents and great costs. For this reason, currently researchers are working on green approaches that are wholly vital for the synthesis of NCPs. Green methods can exhibit many advantages such as being more economical and avoiding the use of organic substances and easy control of the processes. In summary, the successful synthesis of nanocomposites using a green manner has been described from several natural sources, such as *Sambucus nigra* L. [33], *Diospyros kaki* [34], *Eichhornia Crassipes* [35] and the attained produces are suitable for photocatalytic investigations in wastewater treatment. The abundant use of zinc and calcium oxides in medical science and the removal of pollutants led to the synthesis of NCPs using *Caccinia macranthera* extract through a green chemistry approach for the first time. In this research, the aim is to prepare Ag-doped ZnO/CaO nanocomposites by the green method to investigate their photocatalytic properties, cytotoxicity effects, and antibacterial applications. Our new effort involves the application of *C. macranthera* seed extract as a stabilizing and capping agent to control the size and shape of NCPs through the manufacturing process. The structural attributes and morphology of NCPs were studied through the XRD, FTIR, and FESEM/PSA/EDX techniques. Also, the biocompatibility and cytotoxicity of synthesized NCPs were evaluated on Huh-7 cancer cell lines with an MTT test. Furthermore, the photocatalytic activity of NCPs towards the degradation of MB dye under UVA-light was also investigated. Additionally, the outcomes of the broth microdilution method were examined to perceive the antibacterial functionality of NCPs towards gram-positive bacteria and gram-negative bacteria.

Experimental

Merck Co. provided $Ca(NO_3)_2{\bullet}4H_2O$, $Zn(NO_3)_2{\bullet}6H_2O$, and $AgNO_3$ salts (99%). The aqueous extract was prepared using collected fresh *C. macranthera* plant from the Razavi Khorasan province of Iran. The materials needed for the cytotoxicity, antibacterial, and photocatalyst tests were purchased from Merck and Sigma. The Huh-7 cancer cell line was achieved by the Pasteur institute of Iran. Throughout the experiments, the solvent was distilled water.

Caccinia macranthera seed extract preparation

Caccinia macranthera extract was prepared by adding 1 g of completely washed *C. macranthera* seeds to 100 mL of distilled water and stirring for 2 h at 60 °C. The gained extract was filtered with Whatman paper and stored at 4 °C for future use.

Fabrication of Ag-doped ZnO/CaO nanocomposites

The NCPs were manufactured using a green procedure that included zinc, calcium, and silver nitrates as the suppliers of salts and *C. macranthera* seed extract as the capping agent. The first, 20 mL $Zn(NO_3)_2$•$6H_2O$ solution (A, 0.50 M) was added to 20 mL $Ca(NO_3)_2$•$6H_2O$ solution (0.50 M) (Zn to Ca, 1:1). The obtained solution (A) was stirred at 25 °C for 30 min. After, 10 mL $AgNO_3$ solution (10%) was extra to the A solution. In the result, the attained solution (B) was stirred for 40 min. In the continue, 20 mL of *C. macranthera* extract was extra to the B solution and the resulting solution was stirred at 80 °C for 6 h. This method led to the attainment $M(OH)_2$ el, which was dried at 100 °C for 6 h. Then, a calcination routine was performed for 2 h at 700 ºC to achieve the gray-colored NCPs. The biosynthesis plan of NCPs is exhibited in Fig. 1.

Characterization

To validate the synthesized NCP, the samples were characterized using various approaches such as UV–Vis, FTIR, XRD, and FESEM/PSA/EDX. The chemical structure of the compound was checked using FTIR analysis (Shimadzu, model UV-1800). UV–Vis spectrophotometry (Shimadzu, model UV-1800) was used to evaluate the optical properties of NCPs. Furthermore, the crystal structure of NCPs was investigated using the XRD pattern (model, D8-Advance Bruker). Following the estimation of particle size, the morphology and elemental analysis of NCPs were checked using FESEM/EDX/PSA images (Model TESCAN BRNO-Mira3), Afterward, various applications of synthesized NCPs such as antibacterial, anticancer, and photocatalytic activity were investigated.

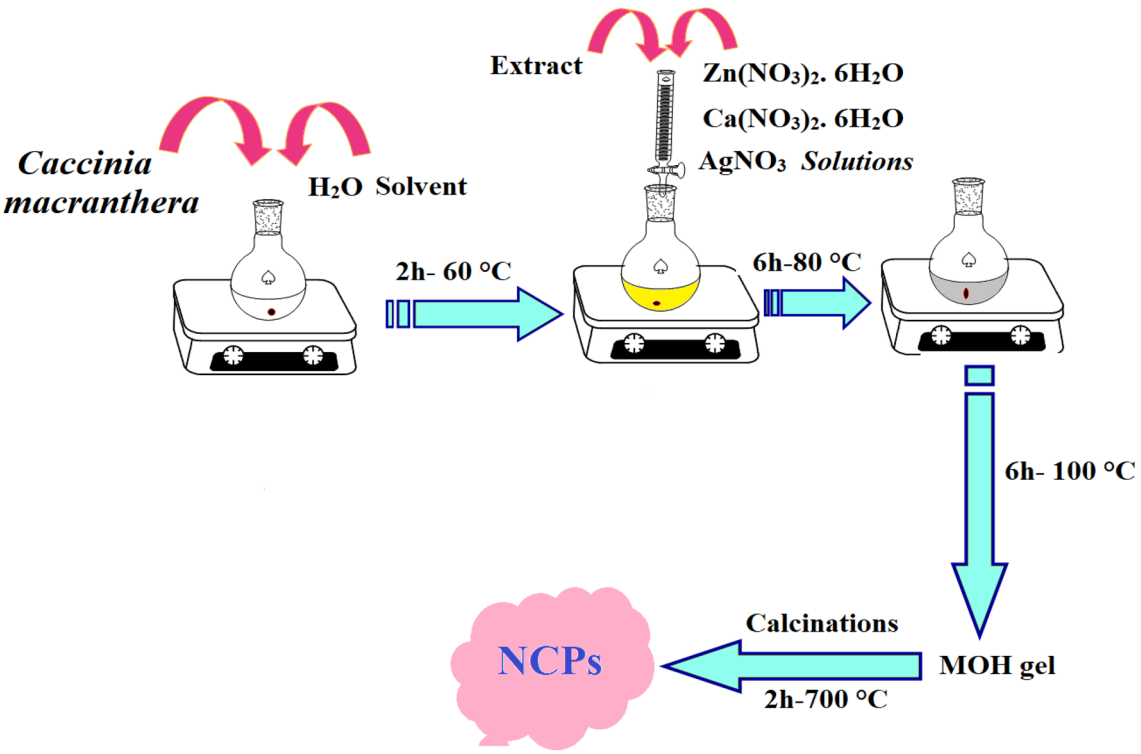

Fig. 1 The green synthesis plan of NCPs

Results and discussion

Photocatalytic activity

One of the chief purposes of this project is to examine the photocatalytic properties of synthesized NCPs in the removal of azo organic contaminants. Therefore, MB dye was selected as an organic contaminant, and the photocatalytic properties of synthesized NCPs were investigated in the degradation process. To evaluate the efficiency of synthesized NCPs in optical degradation of MB dye changes the absorption spectra of the reaction mixture were investigated several times. To obtain the absorption spectrum, the first 100 mL of MB dye solution with a concentration of 1×10^{-5} M was prepared. After making the MB solution and adjusting the pH ~ 10, a certain amount of NCPs (30 mg) was added to it and sonicated for 10 min. Then, the mixture solution was stirred in dark conditions for 45 min to reach the absorption and desorption equilibriums. The resulting solution was then exposed under UV light. During the photocatalytic degradation test of MB dye, about 2 mL of the solution was removed at specified intervals (20 min). In continue, the absorbance of the samples was determined after centrifugation (12,000 rpm) using UV–Vis spectrophotometry at 663 nm. The amount of dye degradation before and after the addition of NCPs was measured and the maximum dye degradation efficiency was calculated using Eq. 1. As can be seen from Fig. 2a, the destruction efficiency decreased with increasing time, so that after 100 min, the degradation efficiency reached about 90%.

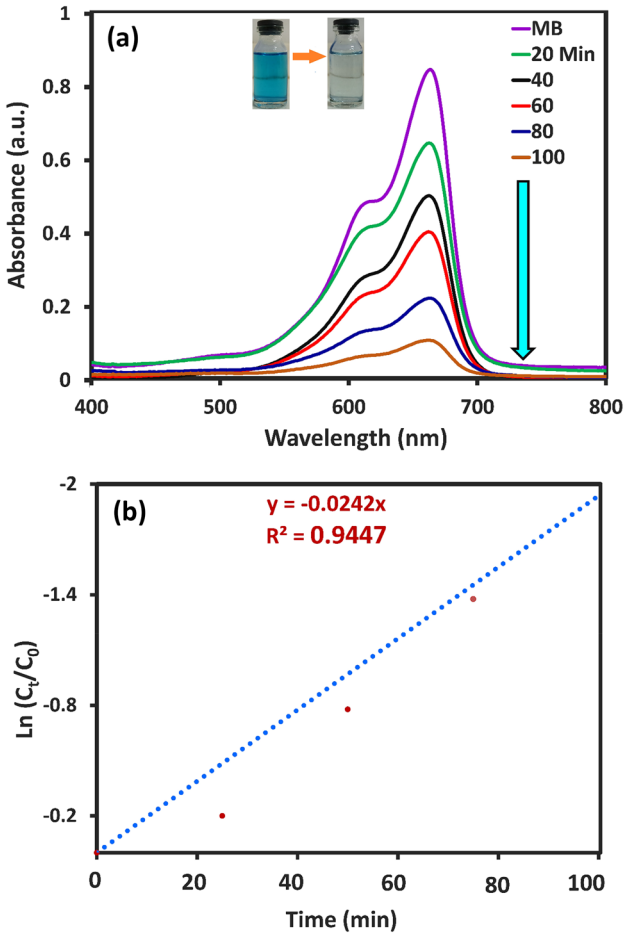

Fig. 2 Photocatalytic diagram of MB dye **a** and kinetic curve **b** of NCPs

$$\text{Degradation}(\%) = \frac{C_0 - C_t}{C_0} \times 100 \quad (1)$$

C_0 = Initial concentrations of the MB dye solution.
C_t = Final concentrations of the MB dye solution.

The reaction kinetics of MB dye degradation was investigated using Eq. 2. The plot of Ln (C_t/C_0) *vs* time is displayed in Fig. 2b. The result shows reaction kinetic is first-order.

$$\text{Ln}\left(\frac{C_t}{C_0}\right) = K_{obs}t \quad (2)$$

where C_0 and C_t are the initial and the final concentration of the dye solution after the passage of time t and k is the kinetic constant of the reaction respectively. The rate constant (K_{obs}) value was obtained to be 0.024 min^{-1}.

The mechanism of photocatalytic reactions is presented in Fig. 3**.** In the following, H_2O molecules react via the holes (h^+) of VB and creation OH° radicals, while the reaction of O_2 with CB electrons leads to the production of $^{\circ}O_2^-$ and the active radicals (H_2O_2, $^{\circ}O_2^-$, OH°) that able to destroy the MB dye in the course of serial chain reactions. The applicability of this method for degrading the MB dye is dependent on the capability of radicals in altering the organic materials into CO_2, H_2O, etc. [17, 36]. The reactions of the photocatalytic test are depicted below (3–7).

$$hv(UV) + NCPs \rightarrow h^+ + e^- \quad (3)$$

$$H_2O + h^+ \rightarrow H^+ + OH^{\circ} \quad (4)$$

$$O_2 + e^- \rightarrow O_2^{\circ -} \quad (5)$$

$$Dye + h^+ \rightarrow Oxidatedproducts \quad (6)$$

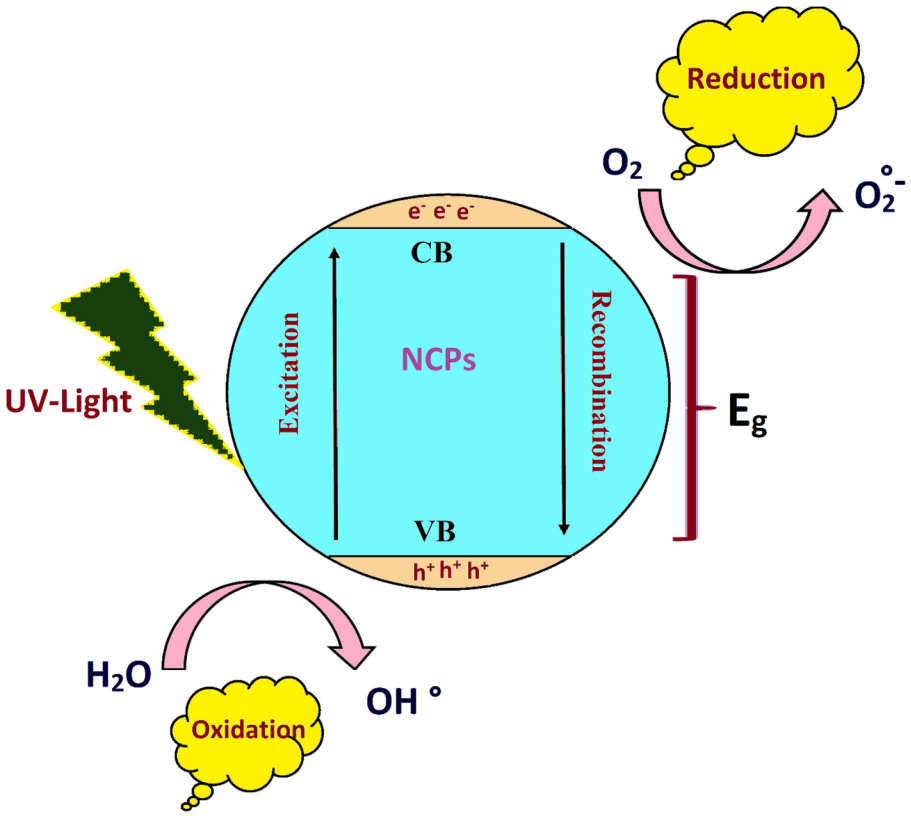

Fig. 3 Mechanism of photocatalytic degradation

$$\text{Dye} + e^- \rightarrow \text{Reductedproducts} \quad (7)$$

Catalyst recovery

A catalyst is a substance that, by participating in a chemical reaction, accelerates it without undergoing chemical changes. That is why catalysts can be used many times, which is economical. At this stage of the project, to evaluate the performance of the prepared photocatalyst, the used photocatalyst in the dye degradation process was collected by centrifugation and washed times several with distilled water and ethanol. The collected sediment was dried at room temperature and applied for reuse in the degradation reaction. Evaluating the efficiency of the collected photocatalyst in the degradation reaction was performed similarly to Photocatalytic activity. The results of dye degradation indicated that the photocatalyst efficiency remained constant in three reuses and reduced in the fourth recovery. The results are reported in Fig. 4.

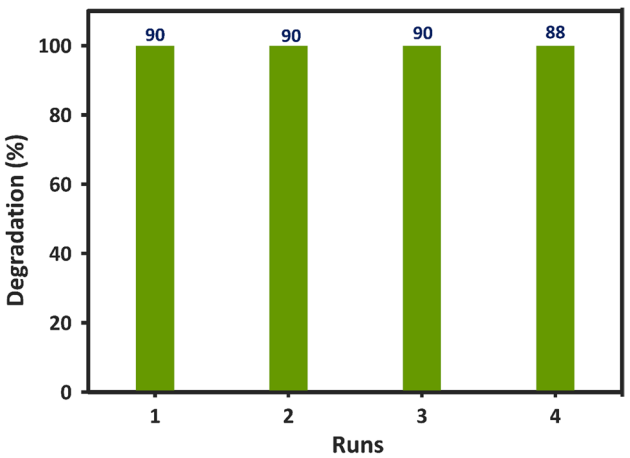

Fig. 4 Recoverability curve of NCPs

Cytotoxicity

The MTT [3-(4,5-Dimethyl-2-thiazolyl)-2,5-diphenyl-2H-tetrazolium bromide (MTT)] test is a colorimetric process for measuring the vital capacity of a cell. It is based on the reduction of tetrazolium yellow crystals by mitochondrial succinate dehydrogenase and the formation of purple crystals of formazan, which are insoluble in water. First, Huh-7 cancer cells were cultured in a DMEM medium containing 10% FBS and 1% antibiotic (100.0 µg/

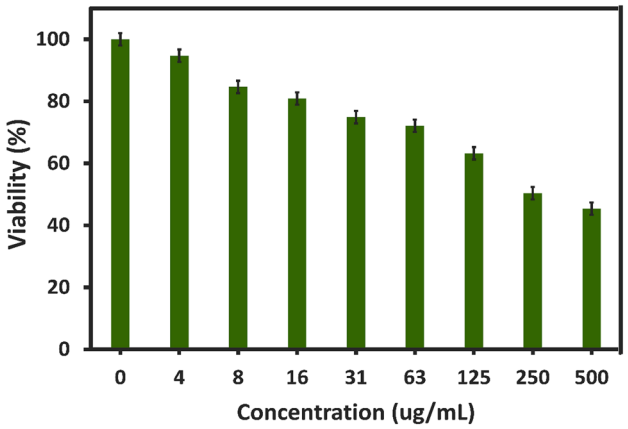

Fig. 5 Evaluation of cell viability by MTT method after 48 h of treatment of NCPs

mL streptomycin/penicillin) and were incubated at 37 °C and 5% CO_2. Then 1×10^4 cells were poured into each of the 96-well plate wells (100 µL). After 24 h, the cells were treated with NCPs at different concentrations (0–500 ppm) for 48 h. Then, the cytotoxicity of nanocomposite on cancer cells was investigated in such a way that after the treatment period, 60 µL of MTT was added to each well and incubated for 4 h. In continue, the MTT was removed and 50 µL of DMSO was extra to each well. The absorbance was scanned at 570 nm by a spectrophotometer. All experimental steps were repeated three times and the viability of cells at each concentration was measured according to the following equation (Eq. 8).

$$\text{Viability}(\%) = \frac{A_t}{A_C} \times 100 \tag{8}$$

A_t = Absorption of the treated sample, A_c = Absorption of the control sample.

The results of the MTT test showed that the synthesized NCPs were able to inhibit the proliferation of cancer Huh-7 cells and in a dose-dependent manner induce cytotoxicity in cancer cells. As shown in Fig. 5, NCPs at concentrations of 0–500 ppm reduce the survival of cancer cells and exert a cytotoxic effect. An examination from the MTT test showed IC_{50} value is about 250 ppm. According to the results of cytotoxicity, these NCPs can be effective on Huh-7 cell lines at high concentrations, which can be suggested as a suitable candidate for biomedical applications.

Antibacterial activity of NCPs

This section implicated the usage of the broth microdilution method to assess the antibacterial functionality of NCPs against gram-positive bacteria *Enterococcus faecalis*

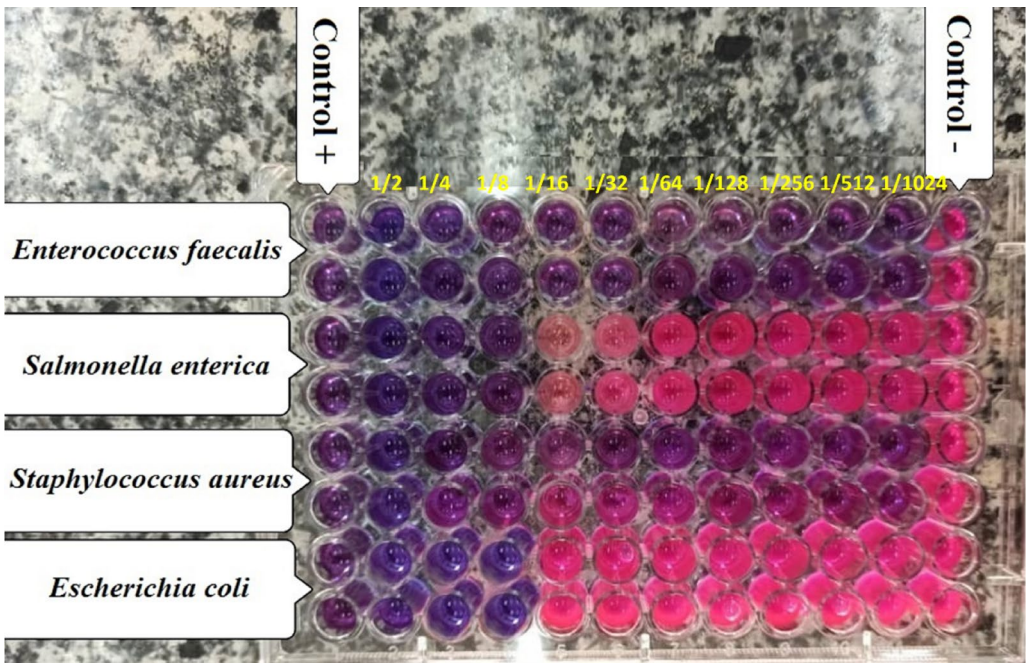

Fig. 6 Assessment of the antibacterial activity of NCPs

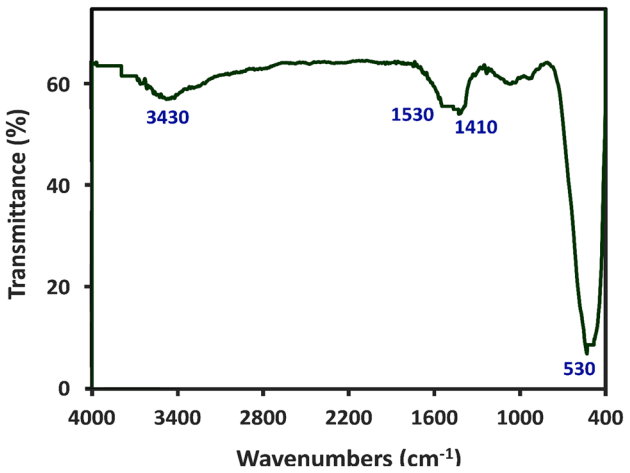

Fig. 7 The FTIR spectrum of NCPs

(ATCC 29212) and *Staphylococcus aureus* (ATCC 29213), and gram-negative bacteria *Escherichia coli* (ATCC 25922) and *Salmonella enterica* (ATCC 14028). Once the growth of strains as the target organisms was completed in the nutrient broth at 37 °C for 24 h, the microbial suspension was arranged by microbial colonies and normal saline while being adjusted to 0.5 McFarland turbidity standard [37]. Subsequently, 100 µL of Mueller Hinton Broth media culture was decanted into every well. The first well of each row was considered a positive control that consisted of a culture medium, chlorhexidine 2% (100 µL), and bacteria (5 µL), whereas the last well of each row was considered a negative control that contained a culture medium and bacteria. In the continuation, next to adding 100 µL of NCPs solution (1000 ppm) to the second well of each row, serial dilution was performed up to the 11th well, which was continued by the addition of 5 µL of diluted microbial suspension equivalent to 0.5 McFarland; the substances were incubated at 37 °C for 24 h. The last well, which was identified with turbidity, was the Minimum Inhibition Concentration (MIC) as the lowest concentration of an antimicrobial with the ability to prevent the visible expansion of a microorganism through an overnight incubation. To better observe the turbidity, 50 µL of resazurin was applied to every well and incubation at 37 °C for 5 h. The antibacterial influence of NCPs (1000 ppm) can be studied by determining the state of turbidity or non-turbidity of the wells to be compared with the control wells. The last well sensed with turbidity was labeled as MIC. The results of investigative the antibacterial activity of NCPs against the bacterial strains are exhibited in Fig. 6. The gathered data indicated that the case of gram-positive bacteria displayed the highest sensitivity to NCPs when compared to the gram-negative bacteria. The MIC values of *E. faecalis* and *S. aureus* are about 0.97 ppm, and *E. coli* and *S. enterica* are about 125 ppm.

FT-IR

The FT-IR was used to determine the functional groups that exist in the compound. The FT-IR diagram of synthesized NCPs is shown in Fig. 7. The identified bands at 470 and 530 cm^{-1} can be ratioed to metal–oxygen (M–O) stretching vibrations, confirming the synthesis of NCPs [38]. Moreover, the stretching and bending vibrations of the O–H group

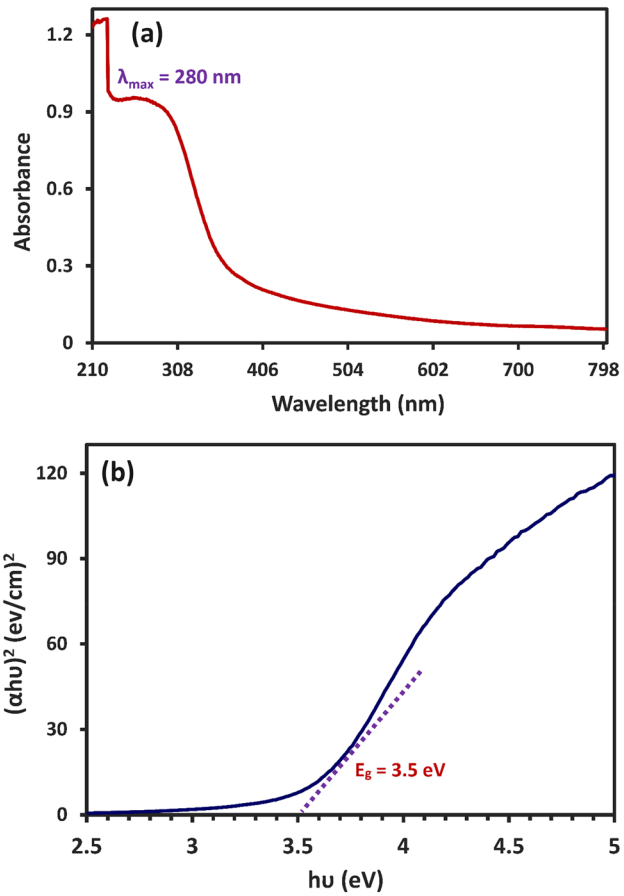

Fig. 8 UV–Vis curve **a** and Bandgap **b** of NCPs

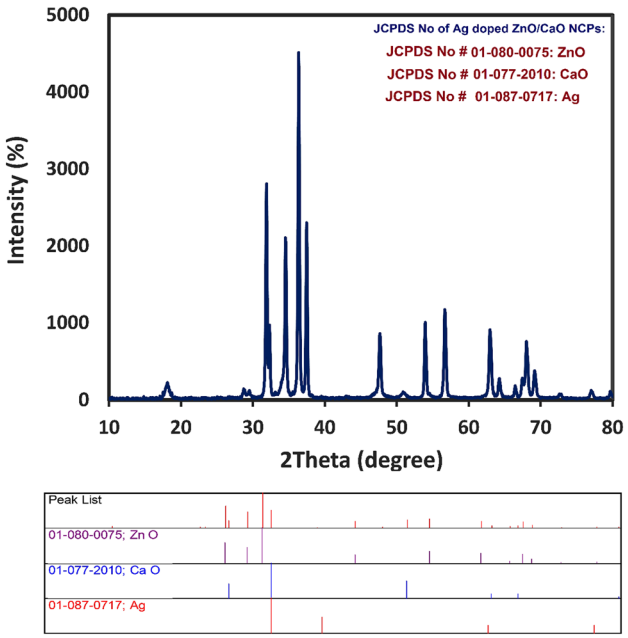

Fig. 9 XRD pattern of NCPs

were detected at 3430 and 1410 cm^{-1}, respectively. The detected peak at 1530 cm^{-1} can be attributed to the residual nitrates, indicating the potential of phytoconstituents in increasing NCP stabilization. [39]. The gathered outcomes conformed to the research of Anand et al. [19] and Wang et al [40].

UV–Vis spectrophotometry

UV–Vis spectrophotometry was used to examine the optical studies of NCPs. The UV–Vis diagram (Fig. 8a) revealed a band at 280 nm, corresponding to the UV zone. Furthermore, the small size and high surface area of NCPs resulted in their powerful ability for photon receiving. The bandgap energy of NCPs was calculated to be around 3.5 eV using the Tauc equation (Eq. 9) [41].

$$(\alpha h\nu)^n = A\left(h\nu - E_g\right) \tag{9}$$

which A is constant, hυ equivalent photon energy (eV), $n=2$ for direct transition and 0.5 for indirect transition. The E_g of NCPs was obtained via extrapolating the linear region of the diagram $(\alpha h\nu)^2$ vs. $h\nu$ (eV) (Fig. 8b).

XRD

The crystallinity of manufactured NCPs was investigated using the XRD spectrum (Fig. 9). All observed bands were associated with the NCPs and confirmed their face-centered cubic (fcc) structure via the Fm^3m space group. The absence of any other bands approved that these nanoparticles successfully were synthesized [42]. These findings were consistent with standard pattern data. The crystallite size of NCPs was obtained using the Scherrer equation (Eq. 10) which was approximately 29 nm.

$$D(\text{nm}) = \frac{k\lambda}{\beta\cos\theta} \tag{10}$$

which $k=0.90$, λ is 0.154 nm, β corresponds to FWHM (Full width at half-maximum), and θ is the angle.

FESEM/EDX/PSA

Corresponding to the FESEM/PSA/EDX images of manufactured NCPs in Fig. 10a–g, the nanocomposites had spherical morphology (Fig. 10a ,c), and their average size was approximately 23–49 nm (Fig. 10d, f). Furthermore, the lack of agglomerated nanocomposites in the FESEM images confirmed the high porosity of our product [12, 20, 43, 44]. The EDX analysis (Fig. 10g) also confirmed the existence of Zn, Ag, Ca, and O elements in the synthesized NCPs. The obtained results agreed with the findings of Arana et al. [45]. Size and morphology are important factors in cytotoxicity, antibacterial, and photocatalytic activity studies [9].

Conclusions

For the first time, the present paper used a green method to synthesize of NCPs using *C. macranthera* seed extract. The results of FESEM, EDX, and XRD studies confirmed the synthesis of NCPs. Furthermore, FT-IR and UV–Vis techniques were applied for examining the optical attributes and determining the functional groups of NCPs. In comparison to previous studies, silver ion doping significantly increased the photocatalytic activity of NCPs to degradation of MB dye. The broth microdilution technique was done to assess the antibacterial effects of NCPs on gram-positive bacteria including *E. faecalis* (ATCC 29212) and *S. aureus* (ATCC 29213), and gram-negative bacteria including *E. coli* (ATCC 25,922) and *S. enterica* (ATCC 14028). The MIC values of *E. faecalis* and *S. aureus* are about 0.97 ppm, and *E. coli* and *S. enterica* are about 125 ppm. Furthermore, the cytotoxicity of NCPs was assessed on Huh-7 cell lines using an MTT test, that revealed concentration-dependent cytotoxicity, and the IC_{50} amount was reported at approximately 250 ppm.

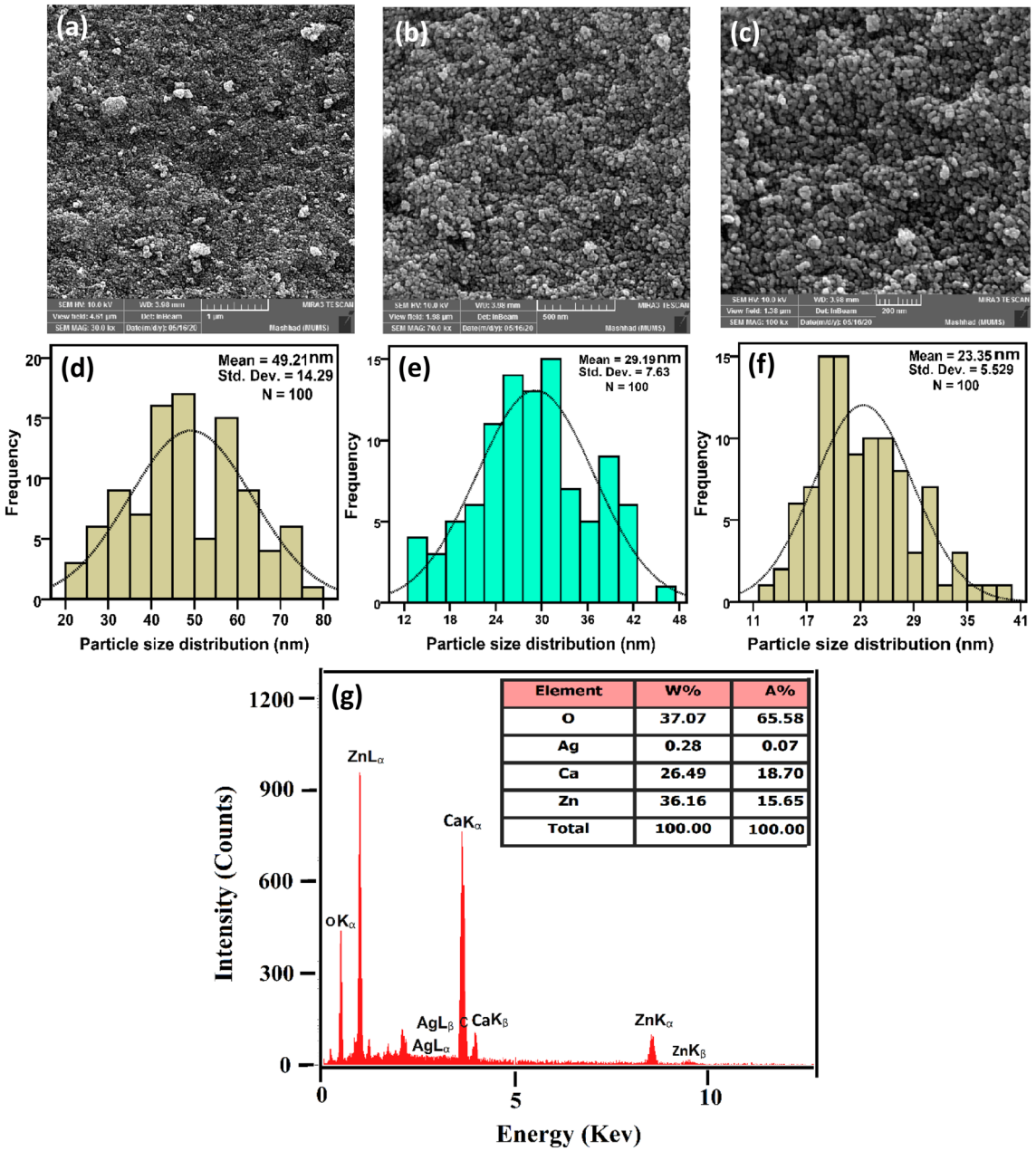

Fig. 10 FESEM (**a**–**c**), PSA (**d**–**f**), and EDX (**g**) of NCPs

Acknowledgements This project was financially supported by the Vice-Chancellor for Research (Grant no. 4001179), Mashhad University of Medical Sciences. This study is the results of a research project and thesis presented by a Post-Doctoral student (Dr. Z. Sabouri).

Author contributions ZS: Investigation, methodology, software, Writing—original draft, formal analysis, SS: data curation, software, writing—review and editing, SSTHM: data curation, writing—review and editing, AM: data curation, writing—review and editing, MSA: data curation, MD: supervision, project administration, validation, methodology, writing-review and editing.

Funding This project was financially supported by the Vice-Chancellor for Research (Grant no. 4001179), Mashhad University of Medical Sciences.

Data availability Not applicable.

Declarations

Conflict of interest The authors declare that they have no conflict of interest.

Ethical approval No experiments are conducted on animals or humans.

References

1. Kannan K, Radhika D, Sadasivuni KK, Reddy KR, Raghu AV (2020) Nanostructured metal oxides and its hybrids for photocatalytic and biomedical applications. Adv Coll Interface Sci 281:102178
2. Villaseñor MJ, Ríos Á (2018) Nanomaterials for water cleaning and desalination, energy production, disinfection, agriculture, and green chemistry. Environ Chem Lett 16:11–34
3. Sabouri Z, Moghaddas SSTH, Mostafapour A, Darroudi M (2022) Biopolymer-template synthesized $CaSO_4$ nanoparticles and evaluation of their photocatalytic activity and cytotoxicity effects. Ceram Int. https://doi.org/10.1016/j.ceramint.2022.02.180
4. Balamurugan S, Balu A, Narasimman V, Selvan G, Usharani K, Srivind J, Suganya M, Manjula N, Rajashree C, Nagarethinam V (2018) Multi metal oxide CdO–Al_2O_3–NiO nanocomposite—synthesis, photocatalytic and magnetic properties. Mater Res Express 6:015022
5. Sabouri Z, Akbari A, Hosseini HA, Hashemzadeh A, Darroudi M (2019) Bio-based synthesized NiO nanoparticles and evaluation of their cellular toxicity and wastewater treatment effects. J Mol Struct 1191:101–109
6. Balamurugan S, Balu AR, Narasimman V, Selvan G, Usharani K, Srivind J, Suganya M, Manjula N, Rajashree C, Nagarethinam VS (2019) Multi metal oxide CdO-Al_2O_3-NiO nanocomposite-synthesis, photocatalytic and magnetic properties. Mater Res Express. https://doi.org/10.1088/2053-1591/aae5af
7. Najjar M, Hosseini HA, Masoudi A, Sabouri Z, Mostafapour A, Khatami M, Darroudi M (2021) Green chemical approach for the synthesis of SnO_2 nanoparticles and its application in photocatalytic degradation of eriochrome Black T dye. Optik 242:167152
8. Akbari A, Sabouri Z, Hosseini HA, Hashemzadeh A, Khatami M, Darroudi M (2020) Effect of nickel oxide nanoparticles as a photocatalyst in dyes degradation and evaluation of effective parameters in their removal from aqueous environments. Inorg Chem Commun 115:107867
9. Sabouri Z, Akbari A, Hosseini HA, Hashemzadeh A, Darroudi M (2019) Eco-friendly biosynthesis of nickel oxide nanoparticles mediated by okra plant extract and investigation of their photocatalytic, magnetic, cytotoxicity, and antibacterial properties. J Clust Sci 30(6):425–434
10. Zhang Q, Xu M, You B, Zhang Q, Yuan H, Ostrikov KK (2018) Oxygen vacancy-mediated ZnO nanoparticle photocatalyst for degradation of methylene blue. Appl Sci 8:353
11. Nagaraju G, Shivaraju G, Banuprakash G, Rangappa D (2017) Photocatalytic activity of ZnO nanoparticles: synthesis via solution combustion method. Mater Today: Proc 4:11700–11705
12. Sabouri Z, Sabouri M, Amiri MS, Khatami M, Darroudi M (2020) Plant-based synthesis of cerium oxide nanoparticles using Rheum turkestanicum extract and evaluation of their cytotoxicity and photocatalytic properties. Mater Technol 37(8):555–568
13. Hamzehloueian M, Sarrafi Y, Darroudi M, Arani MA, Darestani RN, Safari F, Foroumadi A (2022) Synthesis, antibacterial and anticancer activities evaluation of new 4-thiazolidinone-indolin-2-one analogs. Biointerface Res Appl Chem 12:8094–8104
14. Kannan K, Radhika D, Gnanasangeetha D, Lakkaboyana SK, Sadasivuni KK, Gurushankar K, Hanafiah MM (2021) Photocatalytic and antimicrobial properties of microwave synthesized mixed metal oxide nanocomposite. Inorg Chem Commun 125:108429
15. Mousavi SM, Mahjoub AR, Abazari R (2017) Facile green fabrication of nanostructural Ni-doped ZnO hollow sphere as an advanced photocatalytic material for dye degradation. J Mol Liq 242:512–519
16. Manigandan R, Giribabu K, Suresh R, Munusamy S (2014) Characterization and photocatalytic activity of nickel oxide nanoparticles. Int J Chem Tech Res 6:3395–3398
17. Kumar CR, Betageri VS, Nagaraju G, Pujar G, Onkarappa H, Latha M (2020) One-pot green synthesis of ZnO–CuO nanocomposite and their enhanced photocatalytic and antibacterial activity. Adv Nat Sci Nanosci Nanotechnol 11:015009
18. Jamasbi N, Ziarani GM, Mohajer F, Darroudi M, Badiei A, Varma RS, Karimi F (2022) Silica-coated modified magnetic nanoparticles (Fe_3O_4@ SiO_2@$(BuSO_3H)_3$) as an efficient adsorbent for Pd^{2+} removal. Chemosphere. https://doi.org/10.1016/j.chemosphere.2022.135622
19. Anand KV, Keerthika S, Vasantharaja R, Kannan M, Preetha S, Selvan SM, Chaturvedi S, Govindaraju K (2022) Biogenic preparation of ZnO, CaO, and ZnO-CaO nanocomposites and its influence on agro-morphological characteristics of mung bean. Environ Sci Pollut Res Int 29:22251–22259
20. Panchal P, Paul DR, Sharma A, Hooda D, Yadav R, Meena P, Nehra S (2019) Phytoextract mediated ZnO/MgO nanocomposites for photocatalytic and antibacterial activities. J Photochem Photobiol A 385:112049
21. Hooshmand S, Hayat SMG, Ghorbani A, Khatami M, Pakravanan K, Darroudi M (2021) Preparation and applications of superparamagnetic iron oxide nanoparticles in novel drug delivery systems: an overview. Curr Med Chem 28:777–799
22. Hakimi M, Alikhani M (2020) Characterization of α-Fe_2O_3 nanoparticles prepared from a new [Fe (Ofloxacin) $2Cl_2$] precursor: a heterogeneous photocatalyst for removal of methylene Blue and ciprofloxacin in water. J Inorg Organomet Polym Mater 30:504–512
23. Xu X, Chen D, Yi Z, Jiang M, Wang L, Zhou Z, Fan X, Wang Y, Hui D (2013) Antimicrobial mechanism based on H_2O_2 generation at oxygen vacancies in ZnO crystals. Langmuir 29:5573–5580
24. Darroudi M, Iftikhar S, Gaigi H, Taj M, Noor S, Babteen N, Alnajeebi A, Abualnaja M, Raheel A, Bannunah A (2022) Facile synthesis of Fe_3O_4/SiO_2/Cu nanoparticles: investigation of physicochemical attributes of interaction in cationic micellar media and photo-antibacterial impact. Dig J Nanomater Biostruct (DJNB) 17(2):607
25. Sabouri Z, Sabouri S, Moghaddas SSTH, Mostafapour A, Gheibihayat SM, Darroudi M (2022) Plant-based synthesis of Ag-doped ZnO/MgO nanocomposites using *Caccinia macranthera* extract and evaluation of their photocatalytic activity, cytotoxicity, and potential application as a novel sensor for detection of Pb^{2+} ions. Biomass Convers Biorefinery. https://doi.org/10.1007/s13399-022-02907-1
26. Munawar T, Mukhtar F, Yasmeen S, Naveed-ur-Rehman M, Nadeem MS, Riaz M, Mansoor M, Iqbal F (2021) Sunlight-induced photocatalytic degradation of various dyes and bacterial inactivation using CuO–MgO–ZnO nanocomposite. Environ Sci Pollut Res 28:42243–42260
27. Revathi V, Karthik K (2018) Microwave-assisted CdO–ZnO–MgO nanocomposite and its photocatalytic and antibacterial studies. J Mater Sci Mater Electron 29:18519–18530
28. Hosny M, Fawzy M, Eltaweil AS (2022) Green synthesis of bimetallic Ag/ZnO@Biohar nanocomposite for photocatalytic degradation of tetracycline, antibacterial and antioxidant activities. Sci Rep 12:7316
29. Silva RM, Raimundo RA, Fernandes WV, Torres SM, Silva VD, Grilo JP, Morales MA, Macedo DA (2018) Proteic sol-gel synthesis, structure and magnetic properties of Ni/NiO core-shell powders. Ceram Int 44:6152–6156
30. Nakate UT, Patil P, Choudhury S, Kale S (2018) Microwave-assisted synthesis of Co_3O_4 and NiO nanoplates and structural, optical, magnetic characterizations. Nano-Struct Nano-Object 14:66–72

31. Bouremana A, Guittoum A, Hemmous M, Martínez-Blanco D, Gorria P, Blanco J, Benrekaa N (2015) Microstructure, morphology and magnetic properties of Ni nanoparticles synthesized by hydrothermal method. Mater Chem Phys 160:435–439
32. Rahman MA, Radhakrishnan R, Gopalakrishnan R (2018) Structural, optical, magnetic and antibacterial properties of Nd doped NiO nanoparticles prepared by co-precipitation method. J Alloys Compd 742:421–429
33. Cao Y, Dhahad HA, El-Shorbagy MA, Alijani HQ, Zakeri M, Heydari A, Bahonar E, Slouf M, Khatami M, Naderifar M, Iravani S, Khatami S, Dehkordi FF (2021) Green synthesis of bimetallic ZnO–CuO nanoparticles and their cytotoxicity properties. Sci Rep 11:23479
34. Haq S, Raja AW, Rehman SU, Mezni A, Ben Ali M, Hedfi A, Shahzad MI, Rehman W, Shahzad N, Waseem M, Ahmad P (2021) Phytogenic synthesis and characterization of NiO-ZnO nanocomposite for the photodegradation of brilliant green and 4-nitrophenol. J Chem 2021:3475036
35. Aragaw SG, Sabir FK, Andoshe DM, Zelekew OA (2020) Green synthesis of p-Co_3O_4n-ZnO composite catalyst with *Eichhornia crassipes* plant extract mediated for methylene blue degradation under visible light irradiation. Mater Res Express 7:095508
36. Elahi B, Mirzaee M, Darroudi M, Kazemi Oskuee R, Sadri K, Amiri MS (2019) Preparation of cerium oxide nanoparticles in salvia *Macrosiphon boiss* seeds extract and investigation of their photocatalytic activities. Ceram Int 45:4790–4797
37. Andrews J BSAC Working Party Report on Susceptibility Testing (2001) Determination of inhibitory concentrations. J Antimicrob Chemother 48:48–71
38. Balaganesh A, Sengodan R, Ranjithkumar R, Chandarshekar B (2018) Synthesis and characterization of porous calcium oxide nanoparticles (CaO NPs). Int J Innov Technol Explor Eng 2:2278–3075
39. Anantharaman A, Ramalakshmi S, George M (2016) Green synthesis of calcium oxide nanoparticles and its applications. Int J Eng Res Appl 6:27–31
40. Wang L, Liu Y, Peng X, Sun Y, Liu X, Liu H, Lin Q, Sun H, Yang B, Li X (2020) Preparation and characterization of CaO/ZnO core-shell structured nanoparticles. Chem Res Chin Univ 36:970–975
41. Sabouri Z, Rangrazi A, Amiri MS, Khatami M, Darroudi M (2021) Green synthesis of nickel oxide nanoparticles using salvia *hispanica l* (chia) seeds extract and studies of their photocatalytic activity and cytotoxicity effects. Bioprocess Biosyst Eng. https://doi.org/10.1007/s00449-021-02613-8
42. Jayabharathi J, Karunakaran C, Kalaiarasi V, Ramanathan P (2014) Nano ZnO, Cu-doped ZnO, and Ag-doped ZnO assisted generation of light from imidazole. J Photochem Photobiol A 295:1–10
43. Chen P, Wang Y, He S, Wang P, Xu Y, Zhang L (2020) Green synthesis of spherical calcium hydroxide nanoparticles in the presence of tannic acid. Adv Mater Sci Eng 2020:9501897
44. Keihani M, Esmaeili H, Rouhi P (2018) Biodiesel production from chicken fat using nano-calcium oxide catalyst and improving the fuel properties via blending with diesel. Phys Chem Res 6:521–529
45. Toledo Arana J, Torres JJ, Acevedo DF, Illanes CO, Ochoa NA, Pagliero CL (2019) One-step synthesis of CaO-ZnO efficient catalyst for biodiesel production. Int J Chem Eng 2019:1806017